JOURNAL OF AIRCRAFT
Vol. 33, No. 2, March–April 1996

Feasibility of Applying Radio–Acoustic Techniques to Non-Line-of-Sight Sensing

Robert C. Michelson,* Krishan K. Ahuja,† and James A. Scheer‡
Georgia Institute of Technology, Atlanta, Georgia 30332

Geophysicists measure the vertical temperature profile of the atmosphere by tracking the speed of propagation of acoustic waves with radar. A modification of this technique was investigated as having possible application to the detection of non-line-of-sight (NLOS) ground targets while maintaining a very low probability of intercept for the interrogating platform. Essentially, a radar may be made to look around corners. This article describes the feasibility, physical limitations, and possible methods to augment the performance of this novel technique whereby a vehicle can remain fully masked to one side by an obstacle while being able to use radar to look around the masking obstruction. Study results indicate that unaugmented NLOS sensing based on radio–acoustic detection principles is possible with detection probabilities exceeding 90%, but only for ranges of 30–50 m under ideal environmental conditions. This article identifies the primary limitations on range performance and shows that various enhancement techniques can drastically improve the performance of the radio–acoustic NLOS sensor, but not without platform covertness and mobility penalties.

Introduction

IN land battle scenarios, the opponent that reveals himself first will often lose in an ensuing encounter. It is therefore imperative that ground forces conduct their mission without being visible to opposing sensors. Various techniques can be employed to make ground vehicles less observable (camouflage, radar-absorbing materials, exhaust coolers, etc.), but simple tactics such as the use of terrain masking are often a more effective means of increasing the survivability of a ground vehicle than any ectophoretic or deceptive devices. A major drawback with the use of terrain masking is that it tends to work both ways: not only is the masked vehicle hidden from view, but the masking terrain serves to block the sensors on the masked vehicle, thereby effectively blinding it to approaching threats.

Extendible antennas/sensor heads overcome the blocked sensor problem but, if active, must be low-probability-of-intercept systems. Also, these line-of-sight (LOS) sensors can actually be a target designator for hostile antiradiation munitions if they are detected.

An alternate approach is to use bistatic sensors such as remote antennas, unmanned aerial vehicles (UAV) or surveillance aircraft to interrogate the battlefield and report what they see to terrain-masked forces. Unfortunately, this can eliminate the element of surprise, may require air superiority in the region, and precludes the possibility of individual ground vehicles operating autonomously (i.e., without having to rely on assets such as UAVs that may not be under their control).

Non-Line-of-Sight Sensing

A technique is used by geophysicists[1] to measure the temperature profile of the atmosphere from the ground by tracking the speed of propagation of acoustic waves with radar. This technique was investigated as having possible application to the detection of non-line-of-sight (NLOS) targets while maintaining a very low probability of intercept for the interrogating platform. Essentially, a radar may be made to look around corners.

The concept works by creating a three-dimensional acoustic diffraction grating in open air. This is done by horizontally transmitting a plane-wave acoustic signal of known period. The resulting periodic regions of compression and rarefaction in the atmosphere will propagate at a speed proportional to a number of factors, most predominantly temperature and wind speed. If a radar signal of an appropriately chosen wavelength (proportional in length to the acoustic wavelength) is transmitted into the advancing parallel acoustic wave fronts, then a minute amount of energy will be reflected from each wave front. This is illustrated in Fig. 1. By choosing the periods of the acoustic and radar transmissions correctly, the reflected

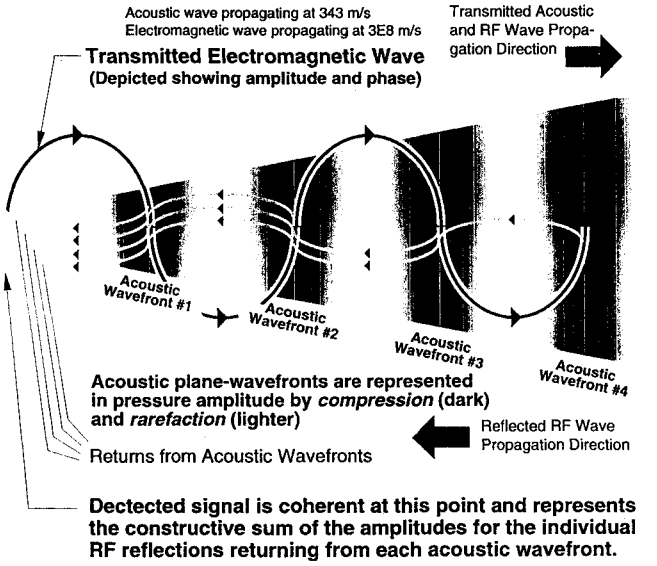

Fig. 1 Relationship between electromagnetic and acoustic wavelengths to achieve coherent constructive summing of returns from individual acoustic wave fronts.

Received Sept. 26, 1993; presented as Paper 93-4344 at the AIAA 15th Aeroacoustics Conference, Long Beach, CA, Oct. 25–27, 1993; revision received Aug. 25, 1995; accepted for publication Aug. 27, 1995.

*Principal Research Engineer, Georgia Tech Research Institute. Member AIAA.

†Professor, Aerospace Engineering; Chief, Acoustics and Aerodynamics Branch, Georgia Tech Research Institute. Associate Fellow AIAA.

‡Principal Research Engineer, Sensors and Electromagnetic Applications Laboratory, Georgia Tech Research Institute.

electromagnetic contribution from each acoustic wave front will add constructively and coherently (Bragg principal) to create a redirected electromagnetic beam propagating at an angle according to Snell's law.

A secondary radar beam is effectively bent backwards to see around the terrain obstacle. Note that the radar and the acoustic generator cannot be colocated or the angle of transmission would equal the angle of reflection (=zero) and the system could only look at itself. If enough acoustic wave fronts contribute to redirect correctly phased electromagnetic energy of sufficient amplitude, then the generated signal will be strong enough to bounce off the target, return by a similar acoustic interaction, and still have enough energy to be detected at the radar receiver. The amount of energy returning to the receiver will be extremely small, and must compete with main-beam energy returns, therefore, such a system would likely have to use range-gating and Doppler discrimination to see targets that are around the corner.

Scanning can be most easily achieved by mechanically moving either (or both) the acoustic or radar source in azimuth/elevation, however, as the angle of the secondary beam diverges away from the acoustic plane–wave normal, more energy will be lost to refractive ducting and noncoherent, nonconstructive summing with the result that the secondary beam will become weaker. In addition, the frequency of either the acoustic source or that of the radar must be swept to maintain the constructive adding of the return signals since the wavelength relationships between the acoustic and radar energy change with the angle of interaction as shown in Fig. 2.

In the unmixed layers of the lower atmosphere, the speed of sound varies significantly when propagating vertically since during the day, and to a greater degree at night, temperature stratification is normally horizontal with respect to the ground.[2] This is one reason why it would be more desirable to look around obstacles rather than over them. Because the wavelength λ varies directly with its speed of propagation (for a fixed frequency f) according to the relationship $\lambda = c/f$, the speed of sound c will be affected by temperature stratification and λ will change. When looking over an obstacle, a pulsed radar interacting with acoustic wave fronts can range-gate on a particular altitude of interest to achieve a specific lookdown angle and range, but it must modify its own frequency of transmission (and therefore its λ) to maximize the amplitude of the returned electromagnetic energy for the temperature at that altitude. The amount of radar frequency slew necessary to match the wavelength of the acoustic energy at a given altitude (temperature stratum) will be directly proportional to various factors such as air temperature, humidity, and wind speed/direction. If, on the other hand, the system is used to look around obstacles instead of over them, then the likelihood of encountering radical temperature variations (due to stratification) over the useful range of propagation is greatly minimized, thereby allowing more precise control of the sensor parameters. The interaction region for the electromagnetic energy and the acoustic plane waves is a finite volume in space described by the intersection of the beams and does not extend to the full range of propagation for the acoustic beam. Therefore, horizontal anomalies created by thermoclines resting in terrain depressions, or temperature and humidity discontinuities encountered by the acoustic beam as it passes over bodies of water, should not be as significant a factor. As a result, surface winds are expected to present a greater source of interaction region disruption than temperature and humidity variations.

Of even greater significance, is that the radio–acoustic interaction region must be large enough to reflect sufficient electromagnetic energy to be detectable by the radar receiver after the full round trip composed of one target bounce and two acoustic interactions. The drawback of increasing the size of the radio–acoustic interaction region is the greater likelihood that temperature- and wind-induced anomalies will be included within the region.

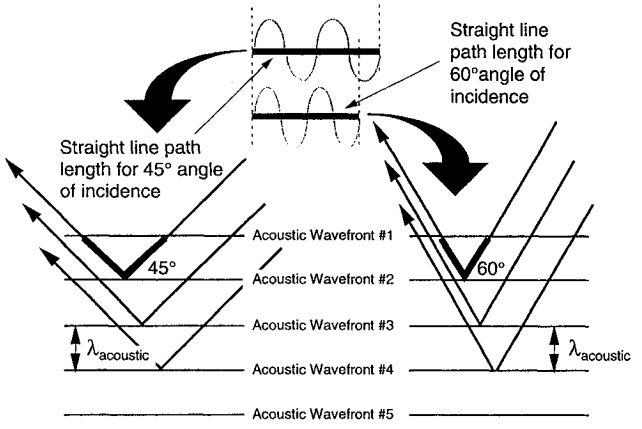

Fig. 2 Examples of angle-induced path length difference requiring change in radar wavelength to maintain coherent adding of reflected rf energy.

An alternative to improving detectability by increasing the radio–acoustic interaction region is to increase the reflectivity of the acoustic wave fronts within the interaction region. This can be done by increasing the acoustic pressure of each wave front by increasing the sound amplitude or by shaping the assumed sinusoidal acoustic waveform to be something with a greater differential pressure change within each cycle (i.e., a square wave). Depending on the acoustic frequency chosen, the difficulty in producing high-amplitude (>100-dB) plane waves will be difficult. Similarly, creating nonlinear waveforms is difficult. The reflectivity of each acoustic pressure wave front can be derived by using the Van Vleck theory of absorption,[3] which relates the degree of attenuation for electromagnetic waves to the presence of atmospheric gases as a function of temperature, pressure, and humidity for a given frequency.

One other alternative to extending the radio–acoustic interaction region is to increase the conductivity of the air by seeding it with a conducting material. Acoustic standing wave energy can be used to organize particulate matter in regular patterns corresponding to points of rarefaction in the standing wave. These methods for increasing the conductivity of the acoustic diffraction grating would result in improved radar performance. The difficulty in maintaining many of these doping conditions or effectively deploying them into the interaction region is not to be underestimated, much less organizing them once they are deployed.

A problem with looking over obstacles instead of around them is that the radiated acoustic and electromagnetic energy will be more easily acquired by loitering antiradiation unmanned aerial vehicles that would then have a direct LOS attack corridor. If, on the other hand, the emissions are horizontal and focused it will be much more difficult for antiradiation drones to acquire them. However, a major drawback with horizontal operation comes from multipath interference and clutter. These mechanisms will tend to hamper target detection and tracking, but they will also make it more difficult for the enemy to find the actual source of the radiated acoustic and electromagnetic emissions. The actual direction of radiation for both the acoustic and primary electromagnetic energy can be directed away from the forward edge of battle and the anticipated ingress direction for target vehicles. Because of multipath reflections from the main acoustic and electromagnetic beams the apparent source of radiation will either be ambiguous or artificial. The radiating platform is never exposed to direct LOS with the target, nor does it radiate any kind of energy directly at the target.

Previous Research

Research in the past has been confined to the study of vertical propagation of co-boresighted radio–acoustic sensor

(RAS) signals for the purpose of atmospheric profiling. The concept of using RAS techniques for a double-bounced angle-skewed rf signal is unique and involves an entirely new area of research. Extensive literature searches and interviews with experts in the field of RAS and radio–acoustic sounding system (RASS) have led the Georgia Tech research team to conclude that the concept described in this article is original and novel. The following paragraphs outline some of the related research that has preceded.

Very little information is available in the literature concerning RAS in general, and nothing is identified regarding its use in an application such as the NLOS sensor. References 1–24 contain articles that are particularly cogent to RAS and RASS as it relates to the subject presented herein.

The White Sands Missile Range (WSMR) and the National Oceanic and Atmospheric Administration (NOAA) facilities at Boulder, Colorado are two of the few operational RASS sites in the U.S. The WSMR's atmospheric profiler research facility consists of three RASS systems: 1) a 50-MHz pulsed unit, 2) a 405-MHz pulsed unit, and 3) a 3-GHz frequency modulated continuous wave (FMCW) unit. All three systems are operational, but two of them are only used as a radar sensor, lacking acoustic sources. The 50-MHz RASS site is fully operational, but only functions in the RASS mode for several minutes an hour. The rest of the time it profiles the atmosphere in a radar-only mode.

The NOAA systems do not use horizontal propagation, they operate from vertical to 15 deg from vertical. NOAA operates a 915-MHz RASS at the Boulder headquarters building that uses a 2-kHz tone for the acoustic signal. At this site, NOAA also gathers and combines data from all 31 wind profiling systems in a nationwide network. The data are available to weather services. Most of these wind-profiling sites are not making heavy use of RASS, if at all, but instead rely mainly on direct radar observations.

Theoretical Reflectivity Analysis

This section deals with the theoretical determination of the electromagnetic reflectivity for free-air acoustically induced compression/rarefaction gradients.

Determination of Received Power for an RASS

When a beam of acoustic radiation with intensity that varies periodically is propagated through the atmosphere, it causes corresponding periodic variations in the atmospheric refractive index. It is well known that electromagnetic radiation will be reflected from a change in refractive index, as shown by the necessity for index-matching camera lenses and dielectric lenses used for microwave applications. The basic principle of the RASS, and also for the NLOS sensor discussed in this article, is this phenomenon of reflection from interfaces of media with differing indices of refraction. In particular, if acoustic radiation of a given wavelength is transmitted, it is found that electromagnetic radiation of wavelength twice that of the acoustic wavelength gives rise to enhanced scattering (Bragg principal). The derivation of the equation for received power from an RASS and the origin of the requirement for enhanced scattering is too long and complex to be given here, but is given in some detail, along with the derivations of some of the other relations used in this article, in the report by Marshall.[25]

Consider the geometry shown in Fig. 3 in which the radar and acoustic sources are collocated. Both transmitters radiate power with a common spherical wave front, so that reflected radar power is focused back on the radar receiver. The total received power P_r can be shown by Eq. (1),

$$P_r = \frac{1.76 \times 10^{-15}\ (\mathrm{m^2/W})\ \pi^3 P_t G_t P_a G_a (1 - \cos\theta/2)^2 n^2 A_r}{64 R^2 \lambda_a^2} \tag{1}$$

where P_t and P_a are the transmitted rf and acoustic power, respectively, and G_t and G_a are the gains of the rf and acoustic transducers. The acoustic beamwidth is θ, R is range, n is the number of cycles the acoustic wave is subtended in space, and λ_a is the wavelength of the acoustic radiation. A_r is the area of the receiver aperture. Note that this equation includes the condition $\lambda = 2\lambda_a$ implicitly. In the next section, this equation will be used in a heuristic derivation of the radar cross section of an acoustically perturbed portion of the atmosphere.

Heuristic Derivation of the Radar Cross Section for Radio–Acoustic Sounding

The radar cross section is a useful target-related parameter that allows one to assess the performance of a radar based on its specifications. This parameter is normally used for radars that illuminate a target that does not fill the transmitter beam, and the spatial distribution of the power reflected from the target is much larger than the receiver aperture. These conditions lead to a $1/R^4$ dependence of power received from the target, where R is target range.

A useful formulation of the radar equation, which shows how this $1/R^4$ dependence arises, has been given by Skolnik,[3] who writes this equation as Eq. (2):

$$P_r = \left(\frac{P_t G_t}{4\pi R^2}\right)\left(\frac{\sigma}{4\pi R^2}\right) A_r \tag{2}$$

In this equation, P_r is the received power, P_t is the transmitted power, G_t is the transmitter antenna gain, σ is the target radar cross section, and A_r is the receiver collecting area. The three factors in this equation represent 1) the power density in the target plane, 2) the fraction of power scattered into the receiver plane, and 3) the receiver collection area, respectively. This formulation of the radar equation neglects atmospheric and system losses for clarity, but these factors can easily be included.

To attain insight in relating the radar cross section for the case discussed previously to that seen by a radar acoustic sounding system, it is necessary to consider the RASS geometry. Figure 3 shows the spherical electromagnetic and acoustic waves propagating outward from a collocated radar and acoustic source. In considering this geometry, note that some fraction of the electromagnetic radiation emitted by the radar will be collected by the collocated radar receiver and that this fraction is just the reflectivity of the acoustically modulated medium multiplied by the transmitted power. In particular, if the medium were 100% reflecting, all of the transmitted power would fall back on the receiver because of the spherical geometry. For this reason, relating the returned power for the RASS case to that for the normal radar case is something of an artifice, but it does provide some insight into the level of signals expected from an RASS as compared to that expected from a radar.

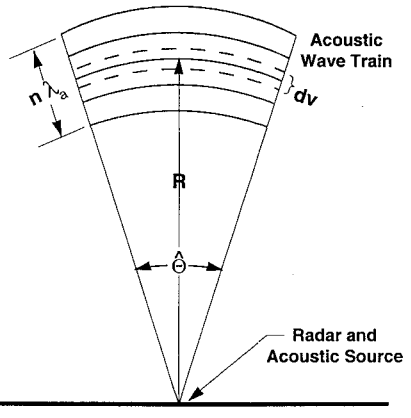

Fig. 3 Scattering geometry for an RASS.

The power received by a radar operating in an RASS mode has been determined by Marshall,[25] who derives Eq. (3):

$$P_r = \frac{P_t G_t}{4\pi R^2} \times \frac{\pi^4(1 - \cos\theta/2)^2 B^2 A^2 n^2}{16\lambda_a^2} \times A_r \qquad (3)$$

The only previously undefined parameters are the constants A and B, the transmitted acoustic power P_a, and the acoustic antenna gain G_a. In deriving this equation, it is assumed that the RASS wavelength convention, which requires that the acoustic wavelength be twice the radar wavelength, is met. Marshall shows Eq. (4),

$$B^2A^2 = 1.76 \times 10^{-15}\ (\mathrm{m^2/W})\ P_aG_a \qquad (4)$$

where the numerical constant has the units m^2/W as indicated. This factor relates the RASS cross section to the transmitted power and the acoustic antenna gain. To arrive at the RASS radar cross section, the center terms of the radar equation formulated by Skolnik and that derived by Marshall are equated in a heuristic way, giving Eq. (5):

$$\sigma = \frac{4\pi^5 R^2(1 - \cos\theta/2)^2 n^2 P_a G_a[1.76 \times 10^{-15}\ (\mathrm{m^2/W})]}{16\lambda_a^2} \qquad (5)$$

It is instructive to make a sample calculation with this equation using the parameters: $R = 1$ km, $n = 100$, $P_a = 100$ W, $G_a = 30$ dB $= 1000$, $\theta = 2\sqrt{\pi/G_a} = 0.112$ rad, and $\lambda_a = 0.1$ m (~3-kHz af). Substitution of these parameters gives an equivalent radar cross section of 0.033 m^2. This fairly low cross section is an indication of the tenuous nature of the acoustically perturbed medium. There is also a reflection mechanism caused by small fluctuations in the index of refraction because of atmospheric turbulence.

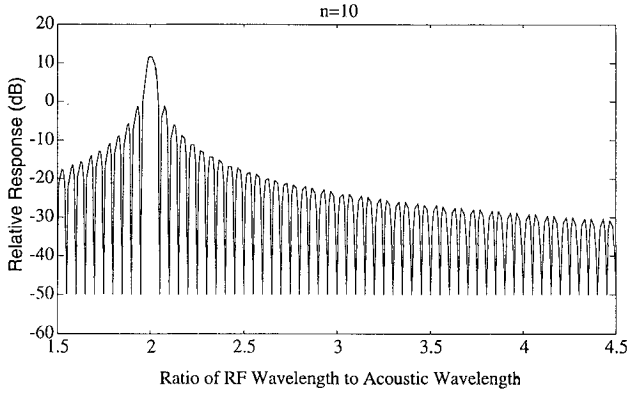

Fig. 4 Relative signal return as a function of wavelength mismatch for acoustic wavelength of 0.1 m and an acoustic pulse length subtending 10 radar wavelengths.

Radar Scattering from Index of Refraction Fluctuations Due to Atmospheric Turbulence

Radar backscatter from atmospheric turbulence has been observed by several workers[26,27] and the theory of this type of scattering has been extensively treated.[28,29] The application of this work has so far been mainly in the area of detection of severe storms and prediction of such strong turbulence effects as wind shear. As might be expected, the scattering from turbulence inhomogeneities is weak and one must resort to careful choice of system parameters and long-term averaging to obtain useful results, especially for long ranges.

The backscattered power received from an atmospheric scattering volume with backscatter coefficient β, measured in m^2 per unit volume is given by Eq. (6) (Ref. 30),

$$P_r = \frac{P_t A_r \beta c \tau}{2R^2} e^{-2\sigma R} \qquad (6)$$

where β is the backscatter coefficient, σ is atmospheric attenuation coefficient, c is the speed of light, and τ is pulse length.

The backscatter coefficient for scattering from turbulence is predictably small because of the tenuous nature of the scattering medium. This coefficient is given by Tatarski[30] as Eq. (7),

$$\beta = 2\pi k^2 \Phi_n(2k) \qquad (7)$$

where k is the wave number and Φ_n is the spatial spectrum of the index fluctuations evaluated for $2k$. This result has the familiar λ^{-4} dependence characteristic of Rayleigh scattering and indicates that shorter wavelengths give more signal return, but the form of the spectral distribution will show that these wavelengths are only marginally better.

A suitable fluctuation spectrum has been suggested by Tatarski[30] and is given by Eq. (8),

$$\Phi_n(k) = 0.033 C_n^2 k^{-11/3} \qquad (8)$$

where C_n^2 is the index of refraction structure parameter. Substituting this expression into the expression for β gives Eq. (9),

$$\beta = 0.0163\pi C_n^2 k^{1/3} \qquad (9)$$

so that the scattering coefficient varies as $\lambda^{-1/3}$ instead of λ^{-4}. This result slightly favors the higher radar frequencies, but is outweighed by the rapid increase in power output available from transmitter tubes as the frequency decreases.

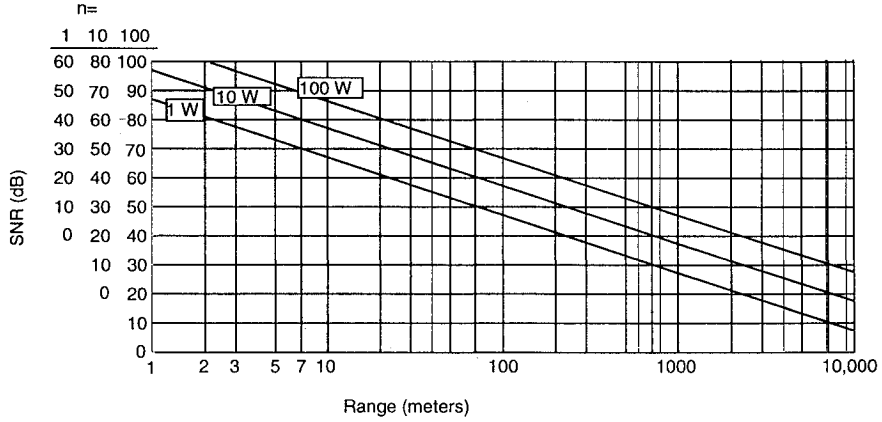

Fig. 5 Plot of RASS SNR for several values of P_t.

Again, it is instructive to make a sample calculation, this time of the expected received power for scattering from atmospheric turbulence. Measurements of the parameter C_n^2 made by Georgia Tech several years ago gave a maximum value of 5×10^{-12} m$^{-2/3}$. Using this value and a radar wavelength of 0.2 m gives a scattering coefficient of 2.58×10^{-12} m^2/m^3. Substituting this value into the equation for backscattered power P_r gives a return power of 1.62×10^{-14} W for a range of 1 km and a pulse width of 67 ns. If one considers that kTB for a matched filter receiver (k is Boltzmann's constant, T is temperature, and B is bandwidth) is 6.21×10^{-14} W, one realizes immediately that basing a NLOS sensor on a turbulence-induced index of refraction fluctuations alone is probably not viable. The use of longer pulses, higher frequencies, and higher transmitter powers will increase the return from turbulence, but an increase in return power based on these changes is probably still not enough to make reflections from naturally occurring atmospheric turbulence useful. (Note that since wind tends to move the acoustic wave train so that it is no longer properly aligned with the radar transmitter and receiver, the effects of offset and wind turbulence are similar. Depending on the nature of the wind, the effect on the acoustic wave phase fronts is to displace them from their central position above the radar antennas and to distort the otherwise spherical shape.)

Deviations from the λ Matching Condition

Since the electromagnetic radiation from a radar scatters from periodic index of refraction variations generated by an acoustic wave, and there is a certain resonance condition $\lambda = 2\lambda_a$ that gives enhanced reflectivity, one would think that this resonance might occur for other wavelength relationships, namely for $\lambda = \lambda_a$, $\lambda = \lambda_a/2$, etc. Despite this strong intuitive inclination, the original condition for which the electromagnetic wavelength is twice as long as the acoustic wavelength is the only one for which resonant reflection occurs. This situation is unfortunate because the system designer for the NLOS sensor is forced to use longer radar wavelengths than desired. There is a practical limit to the acoustic wavelength resulting from the fact that higher acoustic frequencies are severely attenuated in the atmosphere. This condition forces the radar wavelengths to large fractions of a meter with an accompanying decrease in resolution for a given antenna size. This section treats the degradation on sensor performance that occurs if the matching condition $\lambda = 2\lambda_a$ is not met.

In the report that is the definitive work on RASS, Marshall[25] derives the power received from an acoustically perturbed atmosphere for arbitrary values of the ratio of acoustic-to-electromagnetic wavelength. He then divides this power by that obtained for the optimized wavelength relationship to obtain the ratio of these two powers. The result of dividing the power P_r received for an arbitrary electromagnetic wavelength to that received for the case of an optimized wavelength $P_r(2k)$ is given by Eq. (10),

$$\frac{P_r}{P_r(2k)} = \frac{32 \sin^2[2\pi n(k/k_a)]}{n^2\lambda^2}\left[\frac{k_a^2 + 4k^2}{(k_a^2 - 4k^2)^2} - \frac{\cos k_a(R_a + R_b)}{(k_a^2 - 4k^2)}\right] \tag{10}$$

where R_a and R_b are the ranges corresponding to the beginning and end of the acoustic pulse as shown in Fig. 3. Note that this equation is indeterminate (0/0) for $k_a = 2k$ and is of the general form $\sin^2 x/x^2$. The period of the sine function varies with n, so that the requirement for the proper wavelength match becomes more stringent as n increases.

Calculations of the relative power as a function of the ratio of wavelength-to-optimum-wavelength were calculated and the results for $n = 10$ are shown in Fig. 4. This curve clearly shows that the maximum return occurs for $\lambda = 2\lambda_a$. This result places a severe restriction on the implementation of a NLOS sensor, since it forces the radar wavelength toward undesirable longer values, especially since shorter wavelength, higher frequency acoustic waves do not propagate well in the atmosphere.

If a nonsinusoidal acoustical pulse train is generated with the acoustical pulse width adjusted for first-order Bragg reflection and the pulse spacing adjusted for multiple-order Bragg reflection, then the rf wavelength can be small and the acoustical wavelengths can be large. This technique allows both the acoustical and the microwave designs to be optimized for transducer aperture size and power output while maintaining a Bragg-enhanced return.

A pulsed acoustic source with a carefully designed pulse-width-to-interpulse-period can be constructed that will allow the Bragg condition to be matched between the leading and trailing edges of each pulse (on an intrapulse basis), while also allowing the Bragg condition to be matched between the leading or trailing edges of adjacent pulses (on an interpulse basis).

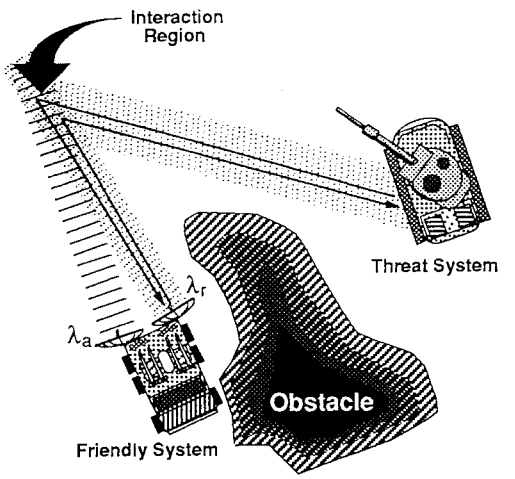

Fig. 6 Case geometry and path definitions.

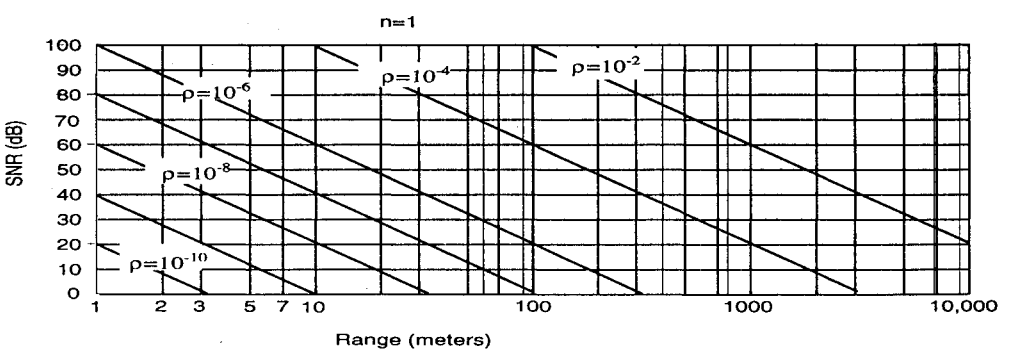

Fig. 7 NLOS performance: rf = 15 GHz, n = 1.

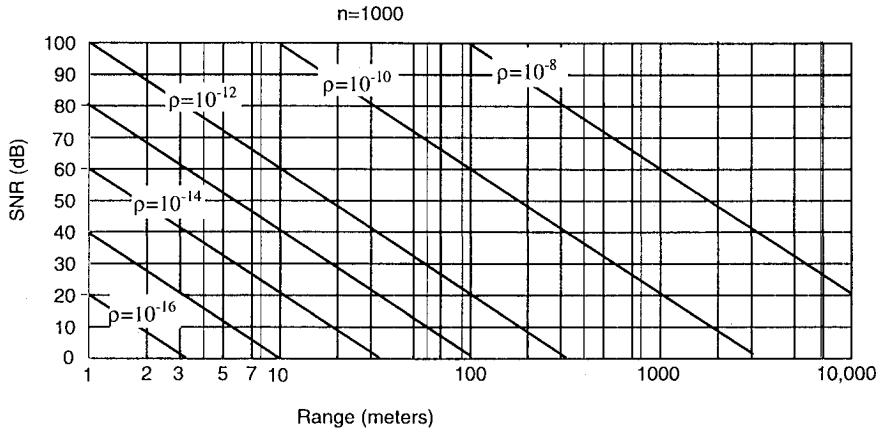

Fig. 8 NLOS performance: rf = 15 GHz, n = 1000.

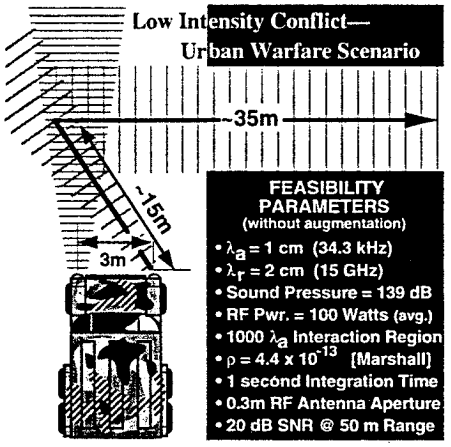

Fig. 9 Baseline NLOS RAS scenario.

This condition can be created for many λ_a and λ_r combinations besides that of $2\lambda_a = \lambda_r$.

The reason this can be done is because the frequency content of the sharply rising and falling edges of the nonlinear acoustic pulse train contain many Fourier component frequencies that correspond to the various side-lobe peaks of Fig. 4. This means that the Bragg-enhanced return will be less energy efficient than that of the simple $2\lambda_a = \lambda_r$ case because of the falloff in enhancement as non-$2\lambda_a = \lambda_r$ contributions from the various side-lobe frequencies of Fig. 4 are coherently summed to form the enhanced return. As stated initially, the advantage of considering this technique is that higher frequency radars can then be used with lower frequency acoustic sources to achieve a degree of Bragg enhancement. The degree of enhancement will be dependent on the frequency content of the nonlinear acoustic pulse train and the energy content of these frequencies.

Since the higher acoustic frequencies will not propagate as well as the lower frequencies, some pre-emphasis might be given to the higher frequencies in order to have the appropriate mix of frequencies and their relative amplitudes by the time they propagate to the interaction region. Such signals could be created at very high sound pressure levels by employing multiple phase-locked sources at different acoustic frequencies to achieve the desired waveform in the interaction region through superposition of the energy from the individual sources.

Detection Performance of RAS

The following analysis provides a perspective on the performance of a RAS system when employed as a NLOS sensor to peer around obstacles. The basic quantity to be determined will be signal-to-noise ratio (SNR), which provides an estimate of how well the NLOS sensor is able to detect targets under various conditions. In particular, the SNR will be calculated as a function of range to the target.

Consider first, the SNR for an RASS system that can be represented by Eq. (11),

$$\mathrm{SNR} = \frac{P_t G_t\, 1.76 \times 10^{-15} \pi^3 P_a G_a (1 - \cos\theta/2)^2 n^2 A_r}{kTBF_n(L_s)64R^2\lambda_a^2} \tag{11}$$

where F_n and L_s represent receiver noise figure and system losses, respectively. In this case R represents range to the target in meters. The acoustic beam angle relative to the radar beam is θ and A_r is the rf aperture area. Figure 5 is a plot of this equation for three values of P_t: 1) 1, 2) 10, and 3) 100 W. It is not unreasonable to use 100-W average power in a mobile radar system. The resulting performance prediction shows that SNR can be expected to be greater than 20 dB out to beyond 10 km, under good conditions, and 5–7 km under moderate conditions. This is consistent with known RASS performance.

The scenario depicted in Fig. 6 is analyzed. A light contingency vehicle (LCV) is attempting to detect a threat vehicle while maintaining masking cover. The concept involves the ability to peer around a corner, detecting a target in a NLOS mode, by using the acoustic wave as a reflector. The assumptions made in this analysis are 1) the acoustic wave approximates a plane wave, 2) 1 s of integration time is used, and 3) the reflection coefficient is determined by the acoustics as given in a previous section.

The received power can be estimated by Eq. (12),

$$P_r = \frac{P_t G^2 \lambda^2 \sigma_t \rho^2}{(4\pi)^3 (R_1 + R_2)^4} \tag{12}$$

where σ_t is the target RCS and ρ is the reflection coefficient.

Using a reflection coefficient values from 10^{-16} to 10^{-1}, the following curves are presented. Solving for the SNR and plotting results in Figs. 7 and 8, for n = 1 and n = 1000 at an rf frequency of 15 GHz, note that for very short ranges (<30 m), the target will be detected for a value of ρ of about 10^{-13}, which could be achieved with state-of-the-art acoustic sources.

Conclusions

Results indicate that unaugmented NLOS sensing based on radio–acoustic detection principles is possible with detection probabilities exceeding 90%, but only for ranges of 30–50 m under ideal environmental conditions. A possible baseline scenario requiring no enhancers is shown in Fig. 9 along with

system characteristics that would lead to this kind of performance under good conditions. This baseline is geared for an urban low-intensity conflict scenario such as that shown in Fig. 9, where a vehicle desires to improve its mobility by being able (while on the move) to look around corners for possible threats prior to crossing blind intersections. Good conditions imply that there is little wind or multipath. In practice, the likelihood of severe multipath exists due to the smooth flat surfaces created by surrounding buildings and pavement. Since this baseline system would operate at short ranges only, the effects of the multipath would be mitigated by having the interaction region only tens of meters in front of the vehicle.

Also, being a short-range scenario, ultrasonic frequencies could be employed with the advantage of covertness and the creation of a good number of acoustic wave fronts within the interaction region. The use of an ultrasonic acoustic source means that a relatively high radar frequency can be used and the radar aperture can be on the order of a square foot, easily accommodated by small vehicles that wish to maintain a low radar cross section themselves.

The primary limitations on range performance derive from the lack of returned signal energy as a result of two factors: 1) the small density gradient existing between regions of sound-compressed and sound-rarefied air and 2) the lack of focusing provided by acoustic plane waves as opposed to that observed in monostatic radio–acoustic sounding scenarios that employ spherical acoustic waves to successfully sense at long ranges (kilometers).

Analyses (beyond the scope of this article) show that various enhancement techniques can drastically improve the performance of the radio–acoustic NLOS sensor, but at the expense of covertness and in some cases, degraded mobility. Alternate techniques to look around corners have been investigated by researchers at the Georgia Tech Research Institute, but most suffer from the necessity to have something physical placed at a known location in front of the interrogating vehicle. Although these alternate techniques are quite viable, they do not have the appeal of the RAS-based NLOS sensor that is instantly deployable and covert. Physical limitations in the state of the art of low-noise radar receivers, high-power (yet compact) acoustic and rf sources, as well as environmental constraints prevent the RAS-based NLOS sensor from being used in long-range applications.

For certain short-range applications the RAS-based NLOS sensor does show promise, especially when no physical reflector can be employed. Such applications will likely not have military application, but will be found in industrial and scientific situations where a short range, unobtrusive, noninvasive NLOS sensor is required. This is particularly true where the environment is controlled such as in test chambers, nuclear facilities, or physical security applications.

Acknowledgments

The authors gratefully acknowledge the support of R. B. Efurd (GTRI) for contributions to RAS enhancement techniques and R. W. McMillan (GTRI) and R. G. Strauch (NOAA Wave Propagation Laboratory) for contributions to understanding the Bragg interaction region. Georgia Tech Graduate Student Bill Kallfelz is recognized for many varied contributions ranging from literature searches to logistics.

References

[1]May, P. T., Strauch, R. G., Moran, K. P., and Ecklund, W. L., "Temperature Sounding by RASS with Wind Profiler Radars: A Preliminary Study," *IEEE Transactions on Geoscience and Remote Sensing*, Vol. 28, No. 1, 1990, pp. 19–27.

[2]Neff, W. D., and Coulter, R. L., "Acoustic Remote Sensing," *Probing the Atmospheric Boundary Layer*, American Meteorological Society, Boston, MA, 1986, pp. 222, 223.

[3]Skolnik, M. I., *Radar Handbook*, McGraw–Hill, New York, 1970, pp. 24-13, 24-14.

[4]Lataitis, R. J., "Signal Power for Radio Acoustic Sounding of Temperature: The Effects of Horizontal Winds, Turbulence, and Vertical Temperature Gradients," *Radio Science*, Vol. 27, No. 3, 1992, pp. 369–385.

[5]Ma, Q., Ishimaru, A., and Kuga, Y., "Scattering and Depolarization of Waves Incident upon a Slab of Random Medium with Refractive Index Different from that of the Surrounding Media," *Radio Science*, Vol. 25, No. 4, 1990, pp. 419–426.

[6]Strauch, R. G., Merritt, D. A., Morgan, K. P., Weber, B. L., and Wuertz, D. B., "Wind Profilers for Support of Flight Operations," *Journal of Aircraft*, Vol. 26, No. 11, 1989, pp. 1009–1015.

[7]Fukushima, M., "Received Signal Characteristics of a Radio Acoustic Sounding System (RASS)," *IECIE Transactions*, Vol. E70, No. 5, 1987, pp. 476–483.

[8]Masuda, Y., "Influence of Wind and Temperature on Height Limit of a Radio Acoustic Sounding System," *Radio Science*, Vol. 23, No. 4, 1988, pp. 647–654.

[9]Masuda, Y., Awaka, J., Okamoto, K., Tsuda, T., Fukao, S., and Kato, S., "Echo Power Loss with RASS (Radio Acoustic Sounding System) to Defocusing Effects by Distorted Acoustic Wave Front," *Radio Science*, Vol. 25, No. 5, 1990, pp. 975–981.

[10]May, P. T., Morgan, K. P., and Strauch, R. G., "Accuracy of RASS Temperature Measurements," *Journal of Applied Meteorology*, Vol. 28, Dec. 1989, pp. 1329–1335.

[11]May, P. T., Strauch, R. G., and Morgan, K. P., "The Altitude Coverage of Temperature Measurements Using RASS with Wind Profiler Radars," *Geophysical Research Letters*, Vol. 15, No. 12, 1988, pp. 1381–1384.

[12]Takahashi, K., Masuda, Y., and Unuiki, H., "Analysis of an Acoustic Wave Front in the Atmosphere to Profile the Temperature and Wind with a Radio Acoustic Sounding System," *Journal of the Radio Research Laboratory*, Vol. 34, No. 142, 1987, pp. 55–70.

[13]Bonino, G., Longhetto, A., Trivero, P., Elisei, G., and Marzorati, A., "Evolution of the Atmospheric Convective Boundary Layer Monitored by the Metric Radio Acoustic Sounding System," *Il Nuovo Cimento*, Vol. 12C, No. 2, 1989, pp. 163–171.

[14]Matuora, N., Masuda, Y., Inuki, H., Kato, S., Fukao, S., Sato, T., and Tsuda, T., "Radio Acoustic Measurement of Temperature Profile in the Troposphere and Stratosphere," *Nature*, Vol. 323, No. 2, 1986, pp. 426–428.

[15]Neiman, P. J., May, P. T., Stankov, B. B., and Shapiro, M. A., "Radio Acoustic Sounding System Observations of an Arctic Front," *Journal of Applied Meteorology*, Vol. 30, June 1991, pp. 881–892.

[16]Anon., *Bulletin of the American Meteorological Society*, Vol. 71, No. 3, 1990, pp. 310–318.

[17]Masuda, Y., Iniki, H., Takashi, K., Takami, T., Sato, T., Fukao, S., and Kato, S., "High Time Resolution Monitoring of Tropospheric Temperature with a Radio Acoustic Sounding System," *Pure and Applied Geophysics*, Vol. 130, Nos. 2/3, 1989, pp. 497–509.

[18]Marshall, J. M., Peterson, A. M., and Barnes, A. A., Jr., "Combined Radar-Acoustic Sounding System," *Applied Optics*, Vol. 11, No. 1, 1972, pp. 108–112.

[19]Bonino, G., "Remote Sensing of Thermal Profile in the Lower Atmosphere by Radio Acoustic System," *Proceedings of the 2nd International Symposium on Remote Sensing of the Atmosphere and Oceans* (Rome, Italy), 1983, pp. 107–114.

[20]Post, M. J., Hall, F. F., Richter, R. A., and Lawrence, T. R., "Aerosol Backscattering Profiles at 10.6 Microns," *Applied Optics*, Vol. 21, No. 13, 1982, pp. 2442–2446.

[21]Perry, B., "Measures of Effectiveness of MMW Defeating Aerosols," Georgia Tech Research Inst., GT-SEAL, Atlanta, GA, April 1989.

[22]Hines, J. R., Eaton, R. D., Hatch, W., and McLaughlin, S., "The U.S. Army Atmospheric Profiler Research Facility: A Preliminary View," *SPIE '92* (Orlando, FL), Society of Photo-Optical Instrumentation Engineers, 1992, pp. 122–130.

[23]Eaton, F. D., Peterson, W. A., Hines, J. R., Peterman, K. R., Good, R. E., Beland, R. R., and Brown, J. H., "Comparisons of VHF Radar, Optical, and Temperature Fluctuation Measurements of C_n^2, r_o, and T_o," *Theoretical and Applied Climatology*, Vol. 39, 1988, pp. 17–29.

[24]Jordan, J. R., and Lataitis, R. J., "Feasibility Study for a Low Altitude Wind and Temperature Profiler," National Oceanic and Atmospheric Administration, National Severe Storms Lab., TM ERL WPL-222, Norman, OK, May 1992.

[25]Marshall, J. M., "A Radio Acoustic Sounding System for the Remote Measurement of Atmospheric Parameters," Air Force Cam-

bridge Research Labs. (CRH), AFCRL-70-0438, Bedford, MA 01730, Aug. 1970.

[26]Zrnić, D. S., Smith, S. D., Witt, A., Rabin, R. M., and Sachidananda, M., "Wind Profiling with Microwave Radars of Stormy and Quiescent Atmospheres," National Oceanic and Atmospheric Administration, National Severe Storms Lab., TM ERL NSSL-98, Norman, OK, Feb. 1986.

[27]Hardy, K. R., and Katz, I., "Probing the Clear Atmosphere with High Power, High Resolution Radars," *Proceedings of the IEEE*, Inst. of Electrical and Electronics Engineers, 1969, pp. 468–480.

[28]Villars, F., and Weisskopf, V. F., "The Scattering of Electromagnetic Waves by Turbulent Atmospheric Fluctuations," *Physical Review*, Vol. 94, No. 2, 1954, pp. 232–240.

[29]Clifford, S. F., and Lataitis, R. J., "Mutual Coherence Function for Line-of-Sight Microwave Propagation Through Atmospheric Turbulence," *Radio Science*, Vol. 20, No. 2, 1985, pp. 221–227.

[30]Tatarski, V. I., *Wave Propagation in a Turbulent Medium*, McGraw–Hill, New York, 1961.